

Ultrasonic Monitoring of Reaction Bonding in Silicon Nitride

M.L. Peterson

Center for Quality Engineering and Failure Prevention

Northwestern University

Evanston, IL 60208-3020 USA

Corresponding author: Mick Peterson
Center for Quality Engineering and Failure Prevention
2137 N. Sheridan Rd.
Evanston, IL 60208-3020

Short Title: Ultrasonic Monitoring of Reaction Bonding

ABSTRACT:

This paper describes a system which uses ultrasonic techniques to monitor the reaction bonding of silicon nitride. Reaction bonding of silicon nitride takes place in a nitrogen atmosphere at temperatures up to 1400°C. As with many sensors used in hostile environments, it is difficult to design the ultrasonic sensor in a way that provides optimal clarity of the signal. The sensing system must be designed within the physical limitations on access to the furnace. Ultrasonic probes which accommodate the limited access to the silicon nitride sample have been designed and ultrasonic signals acquired during processing, albeit with significant noise and complexity in the signal. Signal processing techniques are used which make it possible to measure changes in phase velocity and attenuation during reaction bonding. Because of variability in the measured velocity and attenuation, the method of signal processing presented is applicable to those cases where it is not possible to redesign the probe for optimal clarity of the ultrasonic signal. This technique demonstrates the potential to perform measurements using signals which would have been considered intractable in the past. Data obtained from ultrasonic monitoring is suitable for use as an input to a manufacturing process control feedback loop.

INTRODUCTION:

Interest in reaction bonding of silicon nitride is motivated by the useful characteristics of silicon nitride and ability of the reaction bonding process to produce complex parts efficiently. Silicon nitride shows excellent potential as an engineering ceramic for high temperature applications since it has a low coefficient of thermal expansion and high thermal shock resistance. The reaction bonding process is also ideal for the production of complex parts since the process produces a near net shape part that requires only finish machining. While the alternative process, hot pressing, is well suited for producing ceramic parts with simple shapes, many important applications are dependent on continuing the development of the reaction bonding process. A number of examples of applications for silicon nitride in complex shapes are found in internal combustion engines. Extensive use of ceramic engine parts allows an engine to run at higher temperatures and thus at higher efficiency. Reaction Bonded silicon nitride (RBSN) is an ideal ceramic for use in engine parts such as turbocharger recovery turbines, exhaust valves and cylinder head liners [1].

In spite of the obvious advantages of using silicon nitride, production problems have limited its commercial use. Consistent production of high quality parts has been difficult, because variation in the density of the material preform and impurities in the silicon powder significantly impact reaction bonding. Therefore it is unrealistic to expect that a fixed set of processing parameters can be developed for a particular part. This situation suggests the use of some sort of closed loop process control system. However, a monitoring system must be developed prior to implementing the control system. The development of a method for monitoring the reaction bonding is a significant challenge considering the difficult environment under which the process takes place.

Reaction bonding of silicon nitride occurs in a high temperature atmosphere of nitrogen through an exothermic reaction between silicon and nitrogen:



While the primary reaction occurs between solid silicon and the nitrogen gas, a gas and a liquid phase of the silicon are also present. Reaction bonding takes place at 1150-1400 °C which is near the melting point

of silicon. The reaction rate depends on the temperature and on the concentration of nitrogen. Since the reaction is exothermic and occurs near the melting point of silicon, thermal runaway may occur resulting in melted silicon. An excessively fast reaction rate can also prematurely close off the pore network on the exterior of the part. The pore network is required for diffusion of nitrogen to the interior, and premature closure will result in unreacted silicon. Areas of either unreacted or melted silicon in the finished material reduces the strength of the reaction bonded part. If an insufficient processing temperature is used the reaction may slow or stop, also resulting in unreacted silicon. Since reaction bonding of even thin cross section parts may take ten or more hours at temperature, the energy is a significant factor in the cost of the final part. Thus excessive time at temperature may reduce the cost competitiveness of this material. Given these constraints there is no "safe temperature" at which to perform the processing.

Direct measurement of the reaction rate in the material would be the first choice for the control of this process. Measurements of the elastic modulus and porosity using the ultrasonic wave velocity and attenuation are direct indicators of the critical effects in the material caused by reaction bonding. In this type of system, variation in the raw material and processing variables could be actively compensated for by corrections to the processing temperature and perhaps the nitrogen pressure. Active control of the process could guarantee production of a consistently high quality material.

Related research has been done in two separate areas. The first area is the characterization of RBSN using either immersion or contact ultrasonic methods. The second related area concerns the use of ultrasonic methods and long buffer rods as a means of making measurements in a hostile environment. The most relevant work of the first type was done by Thorp and Bushell [2] and specifically looks at the longitudinal wave velocity in reaction bonded silicon nitride samples removed at different points during processing. This data provides a good basis for quantitative assessment of the accuracy of the in-situ measurements. In-situ ultrasonic monitoring of ceramic sintering was done by Gieske and Frost [3]. These authors looked at ZnO and some superconducting ceramic materials. The present paper is influenced by this work, but extensions are made to the signal processing to improve the accuracy and to increase understanding of the measurements. Because of dispersion of the ultrasonic wave which results from the geometry of the system and, possibly, from dispersion in the

material, additional signal processing is a logical extension to the earlier work. Appropriate signal processing will remove the effects of dispersion from the measured phase velocity change and attenuation change during reaction bonding. If dispersion and other effects are found to be secondary, it is possible that the signal processing could be simplified for use in real time process control. Extensive related work on the use of buffer rods has been done by Jen and co-authors [4, 5, 6, 7], with a particular focus on the reduction of multiple mode excitation. In the present effort the separation of the multiple modes is done using signal processing techniques. The use of signal processing separation is in contrast with the development of modified waveguides by Jen and co-authors. Ultrasonic monitoring at high temperatures has been an area of intermittent interest and progress for quite some time. Earlier measurements of wave speeds in low attenuation materials at elevated temperatures was considered by several different investigators such as E.S. Fisher and C.J. Renken [9] and J.R. Frederick [10]. Only recently, however, have techniques become available in the field of digital signal processing that provide alternative methods of overcoming limitations on the use of buffer rods for process monitoring. An alternative approach is provided by laser methods, although cost and complexity considerations would need to be considered prior to their application to this problem. Either of the new approaches to monitoring can open up opportunities for extension to laboratory and industrial applications.

APPARATUS AND PROCESSING:

The reaction bonding of the silicon preform is carried out using conventional processing techniques. The preform used is a cylinder approximately 3 cm. long and 1 cm. in diameter which has been produced in an isostatic press from commercial silicon powder of nominal 10 μm diameter. The furnace makes use of flowing forming gas (90% N_2 10% H_2) held slightly above atmospheric pressure for the reaction. Forming gas is used rather than pure nitrogen to increase the percentage of material reacting and to encourage the reaction of SiO [11]. The reaction begins during a two hour hold at 1250°C before being brought up to 1350°C for ten to fourteen hours. Final processing occurs during a one hour hold at 1400°C.

The ultrasonic monitoring system consists of 1 MHz. transducers in contact with buffer rods which transmit the ultrasonic energy from the transducers located on the exterior of the furnace to the sample reacting in the high temperature forming gas atmosphere inside the furnace. Six signals are obtained in both pulse-echo and through-transmission modes each time data is acquired during the reaction bonding process. The six signals are deconvolved to remove unwanted effects from the measurements. Digitizing of these six signals is done at rates well above the Nyquist frequency and stored for off line processing. Excitation of the ultrasonic transducers is done using a high energy square wave pulser. While commercial high temperature couplant is used for coupling between the transducer and the buffer rod, the buffer rod to sample interface uses dry coupling. Dry coupling is necessary for the buffer rod to sample interface since a couplant such as metal leaf would inhibit the diffusion of nitrogen from the ends of the sample. The nitrogen diffusion is necessary for reaction bonding to take place in the interior of the sample. In pulse-echo and through-transmission configurations pre-amplifiers with gains of 34dB and 54dB were used respectively. Fig. 1 shows the configuration of the system.

Fused quartz buffer rods are used which results in some performance compromise but has the advantage of keeping the cost of the probe assembly low. Use of commercial high temperature transducers made a water cooling system necessary since the transducers are limited to use below 250°C. The cooling system was sized to keep the transducers well below this temperature since the efficiency of the transducers is degraded at higher temperatures. Motion of the buffer rods is also required for acquisition of a full set of reference signals for calibration. The buffer rods and transducers are withdrawn from the contact with the sample each time data is acquired during reaction bonding. Signals are then obtained from the ultrasonic wave reflected from the free end of the buffer rods. Withdrawal of the buffer rods from the sample when data is not being acquired also reduces cooling of the sample by the monitoring system. Because of physical design constraints on the system, the buffer rods cannot be optimized for transmission of the ultrasonic signal. Design of these waveguides for simplicity of the ultrasonic signal would dictate either a larger or a smaller diameter than the buffer rods which were used. Buffer rods with a diameter of less than one-fifth of a wavelength would simplify the processing of the signals because only one mode with significant amplitude would propagate in the waveguide, the bar mode. The bar mode is also non-

dispersive at low frequencies which would have made signal interpretation quite simple. It was found that insufficient energy was transmitted through small diameter buffer rods for the ultrasonic wave to penetrate the ceramic material, particularly when the material is in its initial, unreacted, state. Larger diameter buffer rods propagate a large number of modes with significant energy. If the buffer rod chosen is of sufficient diameter (more than five wavelengths) the signals transmitted through the buffer rod are separated in time. Separation of the signals from different modes would then simply consist of windowing the signal in the time domain. The larger diameter buffer rods did not, however, fit into the small tube furnace used in this work and would be a significant thermal load on even a large furnace. Similar constraints are seen in the work of other researchers in this area, [3, 8] and have been cited as a significant limitation to practical applications of this technique [11]. The use of signal processing techniques to overcome this limitation, which is presented here, is thus thought to be of importance.

A through-transmission ultrasonic signal from early in the reaction bonding cycle is shown in Fig. 2. The signal shown was taken after the sample had been at reaction temperature for 30 minutes. There is approximately 85 dB. of attenuation as a result of the two dry coupling interfaces and attenuation from the sample. The resulting through transmission ultrasonic signal has a significant noise level. As stated previously the complexity of the signal is a result of multiple modes being excited in the buffer rods. Dispersion of the ultrasonic wave also occurs in the silicon nitride sample and in the buffer rods. However the propagated signal does have a sufficient signal to noise ratio to allow signal processing to be performed.

SIGNAL PROCESSING, MODE SEPARATION:

After signals are acquired using the system described above, significant signal processing must be performed. The signal processing employed has two distinct functions. The purpose of the first step in the signal processing is to measure the amplitude and arrival time of the ultrasonic signal which is propagated as a particular mode in the buffer rods. Foremost in this process is identification and separation of waveguide modes. Once a waveguide mode which has significant energy in all of the signals has been identified, the time of flight at a particular frequency and the amplitude of the signal at that frequency must

be extracted. This information is extracted from all six of the signals obtained at regular intervals in the material processing. The six signals obtained each time data is acquired from the process are used in deconvolution. The second function of the signal processing is to separate the effects of other changes that occur in the system from those changes that occur as a result of reaction bonding in the sample. Other changes in the signal may be a result of heating of the apparatus or changes in contact between the buffer rods and either the transducers or the sample.

Signal processing begins by performing time-frequency decomposition of the signal. A time-frequency method is used since the arrival time of the signal must be measured for a particular frequency in a dispersive system. In addition to the dispersion which results from constraints on the waveguide design, dispersion of the wave may also occur in the ceramic material. The assumption of dispersive material is a more general case which should be considered until it has been proven that simplification is acceptable. Additionally, the shape of the ceramic part may also cause dispersion of the wave. Among the options available for time-frequency analysis the wavelet decomposition is employed since this method uses multi-resolution analysis to obtain the optimal time and frequency resolution for all frequency ranges. From the uncertainty principal it is known [12] that the product of the resolution in frequency (Δf) and time (Δt) is lower bounded by:

$$\Delta t \Delta f \geq \frac{1}{4\pi} \quad (2)$$

Thus satisfying Eq. 2 as an equality is the optimal case when time and frequency information must both be determined. Eq. 2 is satisfied as an equality when a Gaussian windowed signal is used [13]. The accuracy issue becomes important since the limits exist at a level of practical measurement accuracy. For example to obtain a 1 μ s resolution in time, the possible frequency resolution is approximately 80 kHz. This resolution may then be used as a guide to understand the accuracy in the scalogram and to determine how close to the cut-off frequency of the waveguide mode accurate time measurements may be made. The optimally determined arrival time is then used for calculation of the phase velocity of the ultrasonic signal.

In the present work the wavelet function used is the Morlet wavelet. This wavelet function satisfies the conditions of admissibility for the wavelet transformation [13] as well as the optimal conditions noted above. The Morlet wavelet is used because it, like the Fourier transform, has a $\pi/2$

quadrature between the real and imaginary parts. The quadrature allows the signal modulus to be viewed without the oscillations of the underlying signal and wavelet. The phase of this complex valued wavelet may also be useful for determination of the arrival time of the signal. The Morlet wavelet, $\Psi_{a,b}$ is a Gaussian windowed complex exponential as shown in Eq. 3, where "t" is the time variable in the untransformed signal, " τ " is the transformed domain time variable, " ω " is the angular frequency and "a" is a scaling factor.

$$\Psi_{a,\tau} = \left(\sqrt{a}\right)^{-1} \Psi\left[\left(t - \tau\right)/a\right], \quad \Psi = e^{-t^2/2} e^{i\omega t} \quad (3)$$

Computations are done using a digitized signal which was significantly oversampled. Conditions for the wavelet transformation are simplified if an overcomplete set of wavelet functions is used. The overcomplete wavelet function case corresponds to oversampling [13]. From the inner product of the ultrasonic signal, $S(t)$, with the wavelet function at incremental delay times (τ) and frequencies (ω), a joint distribution $P(\tau, \omega)$ (Eq. 4) is produced.

$$P(\tau, \omega) = \sum_{t=-\infty}^{\infty} S(t) \Psi_{a,\tau}(t) \quad (4)$$

This distribution represents a deterministic quantity rather than a random variable as suggested by the terminology. The terminology is a result of mathematical parallels to quantum theory. From the joint distribution a sum over all time at a particular frequency, Eq. 5, may be used to estimate the energy density spectrum at a frequency [14]. This marginal is used in later calculations and is one of the two marginals of the joint distribution.

$$\sum_{\tau=-\infty}^{\infty} P(\tau, \omega) d\tau = |S(\omega)|^2 \quad (5)$$

The joint distribution is used for calculation of the marginals and to understand and visualize changes in the signal during processing of the RBSN. The information from the joint distribution is displayed in an image called a scalogram (a spectrogram in single resolution time-frequency methods). The scalogram is the square magnitude of the wavelet transformed signal or the phase of the transformed signal plotted in two dimensions with axes of frequency and time. Either the amplitude or the phase values are plotted in terms of time and scale (frequency band) in the scalogram. Using the scalogram as a visualization tool, a particular waveguide mode may be observed and frequencies identified for use in further analysis. The

frequencies are chosen based on existence of associated areas of the magnitude scalogram which have significant energy at all times during the material processing. The phase portion of the scalogram may also be useful for observing arrival times and shows the dispersion of the signal graphically.

Once the frequencies which will be considered are selected the next step in the signal processing is the determination of signal arrival time. The arrival times are used for velocity calculations as well as in the calculation of the appropriate marginals to find the power spectrum at the frequency of interest. Although it is in theory possible to obtain arrival time information from the wavelet domain signal, difficulties were encountered in finding a method that is appropriately robust for process monitoring. The need for reliability prompted use of a more standard technique. All signals obtained from the furnace were filtered in the frequency domain using a filter shape which corresponds to the wavelets which were identified earlier. The relative delays of the signals were then calculated using the cross correlation between the filtered signal and a corresponding filtered reference signal which was acquired early in the material processing. A time domain window, $W(t)$, was also applied to the reference signal, $R(t)$, which selects the waveguide mode which will be used for the relative delay calculations. The windowing step was necessary since the relative distance between the signals from the different modes varied as the velocity in the waveguides changed with heating. The window only needs to localize the energy in a particular waveguide mode signal so that a single peak will occur in the cross correlation, so partial inclusion of a second waveguide mode signal is not a problem. The stop band of the window was thus chosen to reduce the amplitude of the signal by only one-half. The cross correlation of the windowed reference signal and the comparison signal is then calculated using a standard definition:

$$C_r(t) = \sum_{\tau=-\infty}^{\infty} R_w(\tau)S(\tau-t), \quad R_w(\tau) = R(\tau)W(\tau) \quad (6)$$

The relative delay of two signals corresponds to the point of maximum amplitude, τ_a , of the cross correlation of the two signals. A relative delay time is found from the cross-correlation for the full suite of the six signals which were obtained each time data was acquired during material processing. The arrival time of the reference signal may be added to the relative delay times obtained using this method to obtain an actual arrival time. However the change in velocity or relative delay rather than absolute velocity is of

primary importance for process monitoring. These relative delay times, which are associated with the frequency band of the filter used, are the basis for the later calculation of the change in elastic modulus or change in phase velocity. The arrival times were also used as a limit for the summation in the attenuation calculations.

To calculate a value for the material attenuation from the ultrasonic signal, the magnitude of the spectrum of the chosen modes must be obtained. The power spectrum for the entire signal may be obtained as a marginal from Eq. 5. However to be consistent in the portion of the signal that is considered, the power spectrum should be obtained only for the waveguide mode or modes which are under consideration. For this purpose the limits of the summation in Eq. 5 are modified. The lower limit is taken as the first point in the acquired signal. The upper bound of the summation is a point which is chosen in the reference signal plus the relative delay obtained from the cross-correlation. The base-line time point in the reference signal is chosen to provide a significant amount of signal power in the summation, thereby improving the signal to noise ratio (the power of the signal divided by the power of the noise). In this case the reference point was chosen to correspond to a time associated with a decrease in the wavelet domain magnitude, thus selecting a point between the waveguide mode maxima. The power spectrum for a consistent portion of the signal and for a particular frequency is then defined as:

$$|S(\omega)|^2 = \sum_{\tau=-\infty}^{\tau_a} P(\tau, \omega) \quad (7)$$

From these two steps in the signal processing an arrival time for the waveguide mode of interest is obtained and the power of that mode for a particular frequency is calculated. The remaining step in processing is to deconvolve the effects of changes which occur in the ultrasonic signal as a result of changes in the system other than those effects caused by reaction bonding of the silicon nitride.

SIGNAL PROCESSING, DECONVOLUTION:

Deconvolution of the signal is required since a large number of parts in the ultrasonic system are affected by heat and other changes which occur during the reaction bonding. The deconvolution

separates the response of the material from these other effects. Examples of the effects that are accounted for are the variation in coupling between the buffer rods and the transducer, variation in coupling between the buffer rod and the silicon nitride sample, changes in wave speed or attenuation in the buffer rod and changes in the response characteristics of the piezoelectric transducer which result from heating.

The form of the deconvolution is developed using arguments derived from a physical understanding of significant sources of change in the response of the experimental system. For this discussion the magnitude and the phase of the spectrum of corresponding signals is known from the first step in the signal processing. Thus the arguments are made using the assumption that comparable frequency domain signals are available for each signal. Fig. 3 shows the six signals which were used in the deconvolution. It is assumed that the six signals were all obtained at a single point in time with the system kept at a single temperature. This assumption is thought to be valid in light of the time scale of the changes in the material being quite long and it is thus assumed that the response of the system does not change during this time period. In mathematical form the signals may be shown as the convolution of the contributing response functions (multiplication in the frequency domain).

$$X = A_{1r}(\omega)H_{tb}(\omega)H_b(\omega)T_{bs}H_s(\omega)T_{sb}H'_b(\omega)H'_{bt}(\omega)A_{2r}(\omega) \quad (8a)$$

$$Y = A_{1r}(\omega)H_{tb}(\omega)H_b(\omega)R_{bs}H_b(\omega)H_{bt}(\omega)A_{1r}(\omega) \quad (8b)$$

$$Z = A_{1r}(\omega)H_{tb}(\omega)H_b(\omega)R_{b0}H_b(\omega)H_{bt}(\omega)A_{1r}(\omega) \quad (8c)$$

Where:

$A_n(\omega)$ = Response Spectrum of Transducer n (Transmit or Receive mode respectively).

$H_{tb}(\omega)$ = Spectrum of Coupling Response from Transducer to Buffer Rod.

$H_b(\omega)$ = Spectrum of Response of Buffer Rod.

$T_{bs}(\omega)$ = Spectrum of Transmission Response of Dry Coupling Between Buffer Rod and Sample.

$R_{bs}(\omega)$ = Spectrum of Reflection Response of Dry Coupling Between Buffer Rod and Sample.

$R_{b0}(\omega)$ = Spectrum of Reflection Response of Free End of Buffer Rod (assumed equal to -1).

$H_s(\omega)$ = Spectrum of Response of Sample.

The signal X is produced by one ultrasonic transducer, transmitted through the sample material, and received by the other transducer which is placed at the opposite end of the furnace. In signals Y and Z a single transducer serves as both transmitter and receiver. The received signal Y is reflected from the interface between the buffer rod and the sample material. Signal Z is acquired with the buffer rod withdrawn from contact with the sample and is a reflection from the free end of the buffer rod. The X' signal differs from the X signal only in that the transmitting and receiving transducers are reversed. The Y' differs from the Y and the Z' differs from the Z in that they are taken from different ends of the fixture arrangement, using one transducers as both transmitter and receiver. The goal of the deconvolution is to use a series of reference signals to separate the response of the silicon $H_s(\omega)$.

Solving Eq. 8 for the response of the material ($H_s(\omega)$) a deconvolution formula of the following form is obtained:

$$H_s(\omega) = \sqrt{\frac{X(\omega)X'(\omega)/Z(\omega)Z'(\omega)}{\left[1 - |Y(\omega)/Z(\omega)|^2\right]\left[1 - |Y'(\omega)/Z'(\omega)|^2\right]}} \quad (9)$$

The amplitude of H_s is the attenuation of the through transmission signal with other effects from the system removed. Similarly, the phase of H_s is the time delay as a result of the silicon sample. To clarify the signal deconvolution the phase and magnitude may be written separately as:

$$H_s(\omega) = \sqrt{\frac{|X(\omega)||X'(\omega)|/|Z(\omega)||Z'(\omega)|}{\left[1 - |Y(\omega)/Z(\omega)|^2\right]\left[1 - |Y'(\omega)/Z'(\omega)|^2\right]}} e^{\left(\frac{\phi_x + \phi_{x'} - \phi_z - \phi_{z'}}{2}\right)} \quad (10)$$

The separated form of the equation is more intuitive since the deconvolution of the phase may be recognized as twice the time delay in the buffer rods subtracted from the sum of the time delay of signals going both directions through the entire test fixture.

In Eq. 10 the denominator of the amplitude portion of the deconvolution contains two factors that are squared and subtracted from 1. The subtracted terms themselves are very nearly equal to one since most of the signal is reflected from the dry contact interface, causing the denominator to approach zero and resulting in numerical instability. The numerical instability of the deconvolution makes this operation particularly sensitive to the signal to noise ratio. This numerical instability may be reduced

through use of Wiener deconvolution. Most of the benefits of Wiener deconvolution may be obtained by using the simpler pseudo-Wiener deconvolution [15], the method which will be followed in this case. Only the magnitude of the signal is unstable so the deconvolution of the phase may be directly implemented as in Eq. 10. A deconvolution filter for the magnitude is then defined from Eq. 9 as:

$$K(\omega) = \frac{1/|Z(\omega)||Z'(\omega)|}{\left[1 - |Y(\omega)/Z(\omega)|^2\right] \left[1 - |Y'(\omega)/Z'(\omega)|^2\right]} \quad (11)$$

A fraction of the maximum power in the spectrum (a constant) is substituted for the power spectrum of the noise which is used in Wiener deconvolution. The deconvolution then takes the form:

$$|H_s^{pw}(\omega)| = \sqrt{\frac{|X(\omega)||X'(\omega)||K(\omega)|}{|K(\omega)|^2 + A}} \quad (12a)$$

where:

$$A = C \left[\max |K(\omega)| \right] \quad 0 \leq C \leq 1 \quad (12b)$$

with H_s^{pw} , which is defined like H_s above made more numerically stable. From the mode separation and deconvolution processes, a meaningful value for the changes in amplitude and velocity of the ultrasonic signal may then be obtained.

IV. RESULTS AND DISCUSSION

To verify the accuracy of this technique the change in wave velocity as a function of temperature was measured for a sample of polycrystalline high purity nickel. Published values for the change in Young's modulus as a function of temperature are compared to the results obtained by the method of this paper in Fig. 4. The published values followed current practice for using ultrasonic methods for obtaining velocity information at high temperatures. This method depends on the existence of a clear back wall echo for velocity calculations[16]. The traditional method as seen in Fig. 4 appears to produce a higher accuracy in the measurements, however it is only suitable for low attenuation specimens of a size which is sufficient to allow reflections from the front, back and sides of the sample to be separated in time. Overall trends appear to be reproduced in the current work however and restrictions on the size of the sample are eliminated. If the results from the previous work are accepted as accurate, this measurement provides some

idea of the accuracy of the current method. The results at higher temperatures appear to be somewhat better which may be due to better temperature stability of the furnace at these temperatures. Coupling at the dry contacts also improves at higher temperatures since the quartz buffer rods are approaching their softening temperature. While the current method allows attenuation measurements to be obtained, no other suitable results are available for comparison.

The first representation of the results for the processing of the RBSN are shown in Figs. 5 and 6 as scalograms. While a full discussion of the potential for wavelet methods is beyond the scope of this paper, a few observations should be made regarding the scalogram representation of the ultrasonic data. Since the Morlet wavelet is complex valued either the phase or the magnitude can be plotted as a function of time and frequency in the scalogram. The magnitude scalograms are plotted as wire grid surfaces with the corresponding contour plot shown as a lower surface. Fig. 5 shows the magnitude scalograms from waves transmitted through the sample early and late in the processing of silicon nitride. These figures show quite clearly the peaks in the amplitude associated with the arrival of three different waveguide modes. From these figures it is also clear that the majority of the signal energy is propagated at frequencies near 650 kHz even though the center frequency of the transducer is 1 MHz.

Figure 6 shows both the phase and magnitude of the wavelet coefficients plotted as a function of time and frequency for the same signal shown in the top image of figure 5. While the magnitude is shown as both a wire frame surface and contour lines, the phase is plotted only as contour lines. The phase may be plotted as simple contour lines since the phase is of a geometrically simpler form, the value changes consistently with time. The phase is useful for observing the early arrival of frequencies which have insufficient energy to be observed in the magnitude scalogram. The earliest arrivals at high frequencies propagate at a velocity which approaches the longitudinal wave speed in an unbounded solid. The sensitivity to low amplitude signals also makes the use of the phase to detect the first signal arrival excessively sensitive to noise in the first part of the signal. No suitable technique has thus far been found which allows the phase to be used without interference from noise. Fitting a surface to the phase using a least squares error criterion has shown potential although it requires significant processing time. The development of a technique to use the wavelet phase to obtain phase velocity information would produce

broadband results. However the cross-correlation technique appears to be a good alternative for individual frequency bands.

Further development of the multi-mode waveguide monitoring method could also make use of the multiple waveguide modes to characterize the ceramic more completely. Since different modes correspond to different displacements through the radius of the sample, each mode would be sensitive to pore distributions in a somewhat different portion of the sample. The spectrum of the signal for different modes then contains unique information on the pore distribution of the sample through the radius of the sample. Putting this data into a usable form would, however, be quite complex. Instead an average value for the porosity distribution is obtained by using the scalogram to select a mode and a frequency range with significant energy for which further analysis will be performed. A wavelet center frequency of 650 kHz and the first two modes in figure 5 are chosen for the analysis. This choices of modes and frequency provides sufficient energy in the summation used for calculating the marginal and in the subsequent deconvolution calculation.

Further synthesis of the data at the frequency chosen from the scalogram results in the velocity and attenuation results shown in Fig. 7 and Fig. 8 respectively. The monitoring method shows a clear sensitivity to changes in the material using either the amplitude or the time delay as a measurement variable. The change in time delay, or the change in velocity, is generally considered to be less sensitive to error since velocity measurements involve simpler signal processing. The total 35% increase in velocity obtained from measurements taken from sample 3C during the processing corresponds to a sample weight gain from the reaction of approximately 57% of theoretical. This result is nearly identical to the 34% increase in velocity which was observed during ex-situ testing for a similar sample weight gain [2]. Results are also shown for a second sample, 5C, which shows a significantly different pattern of velocity change during the reaction bonding process. While sample 5C was processed using the same heating schedule as that used for 3C, a faster reaction took place which resulted in a less fully reacted material. A less complete reaction may be observed from the reduced final velocity increase. In spite of the advantages noted for using velocity measurements, the attenuation measurements are also useful for identification of changes which occur later in the processing cycle and measurement of the reaction rate as seen in Fig. 8.

While the velocity measurements saturate early in the processing, changes continue to take place in the amplitude of the signal. This is not a surprising observation since the peak velocity may be obtained when only a small volume of the sample has reacted which provides an acoustic path of reacted material through the sample. Attenuation measurements continue to change as a result of an increase in the reacted portion of the sample which provides the high velocity acoustic path. As in the velocity results, the lower level of reaction in sample 5C may be observed from the reduction in the change in final amplitude of the signal compared to the signal from sample 3C.

Correlation of observations during different stages in the processing with changes in the attenuation and velocity should also be made. This is the next step for application of the system developed in this work, since verification of the interpretation of transitions in the amplitude and the velocity should be made. Accuracy of the results presented is verified through comparison to the change in elastic modulus in nickel and the comparison to ex-situ measurements of velocity change in RBSN. The application of this technique has potential to both advance the basic understanding of the reaction bonding process and to develop a method of providing process control.

CONCLUSIONS:

From the results presented for measurement of velocity and attenuation several key points should be noted. First, even when the waveguide used in an ultrasonic probe cannot be optimally designed, it is possible to use appropriate signal processing methods to measure the attenuation and velocity in a material at high temperatures. However, when it is possible to redesign the waveguide, velocity measurements may be made with greater ease and, possibly, accuracy by using a single mode buffer rod. Regardless of waveguide design, it is possible to measure trends in ultrasonic attenuation and velocity even under the most extreme conditions. The observations of these trends allows future work to focus on the most important parts of the problem where a suitably accurate approach may be applied. In particular, the results from the measurements on reaction bonding of silicon nitride indicate that the measurement of attenuation is extremely important. While measurement of attenuation is more difficult than velocity, it is more sensitive to changes in the material later in the processing when control and monitoring is very

important. Even a point measurement of velocity using laser generated surface waves would not completely overcome this limitation on velocity measurements since the velocity would still be likely to be measured based on waves which propagate only through an outer shell of reacted material.

It is clear from these results for velocity and attenuation of the silicon nitride that a measurable change may be observed during reaction bonding. Use of this information for process monitoring is not constrained by the complexity of the signal processing used, since the time scale of reaction bonding is on the order of tens of hours. The signal processing required for a feedback process control system could thus be implemented using a low cost personal computer even if the calculations required several minutes. Streamlining of the signal processing and implementation of a standardized procedure could also be used to produce results for even faster types of real time monitoring systems. The signal processing methods presented here also help to show some of the potential for error if excessively simplified methods are utilized. Given the interest in this material for use in large scale production, further development and production hardening of this technique could help speed progress in industrial application of reaction bonding silicon nitride.

REFERENCES:

- 1: S.A.E. *Automotive Engineering* 100:29-33 (July 1992)
- 2: J.S. Thorpe and T.G. Bushell. *J. Mater. Sci.* 20: 2265-2274 (1985)
- 3: J.H. Gieske and H.M. Frost. In *Review of Progress in Quantitative NDE, 8B*, edited by D.O. Thompson and D.E. Chimenti, Plenum Press, NY (1982)
- 4: C.K. Jen, L. Piche and J.F. Bussiere. *J. Acoust. Soc. Am.* 88: 23-25 (1990)
- 5: C.K. Jen, C. Neron, E.L. Adler, G.W. Farnell, J. Kushibiki and K. Abe. In *Proc. IEEE 1990 Ultrasonics Symposium*, (1991)
- 6: C.K. Jen, A. Safaai-Jazi, J.C.H. Yu, C. Neron, G. Perluzzo and Z. Wang. In *Review of Progress in Quantitative NDE, 10A*, edited by D.O. Thompson and D.E. Chimenti, Plenum Press, NY (1991)
- 7: C.K. Jen, Ph. de Heering, P. Sutcliffe and J. Bussiere. *Mater. Eval.* 49:701-706 (1991)
- 8: E.S. Fisher and C.J. Renken. *Phys. Rev.* 135:A482-A494 (1964)
- 9: J.R. Frederick. *J. Acoust. Soc. Am.* 20: 586-590 (1948)
- 10: W.M. Lindley, D.P. Elias, B.F. Jones and K.C. Pitman. *J. Mater. Sci.* 14: 70-85 (1979)

- 11: L.C. Lynnworth. *Ultrasonic Measurements for Process Control*, Academic Press, Boston (1989)
- 12: L. Cohen, *Proc. IEEE* 77:941-981 (1989)
- 13: O. Rioul and M. Vetterli. *IEEE Signal Processing Mag.* Oct.:14-38 (1991)
- 14: M. Farge. *Annual Review of Fluid Mechanics* 24:395-457 (1992)
- 15: P. Karpur, B.G. Frock and P.K.Bhagat. *Mater. Eval.* 48:1374-1379 (1990)
- 16: S. Takahashi and E. Yamamoto. *J. Jpn. Inst. Metals* 37:373-375 (1973)

ACKNOWLEDGMENTS

The guidance and support of Professor J.D. Achenbach, advisor for this work, is gratefully acknowledged.

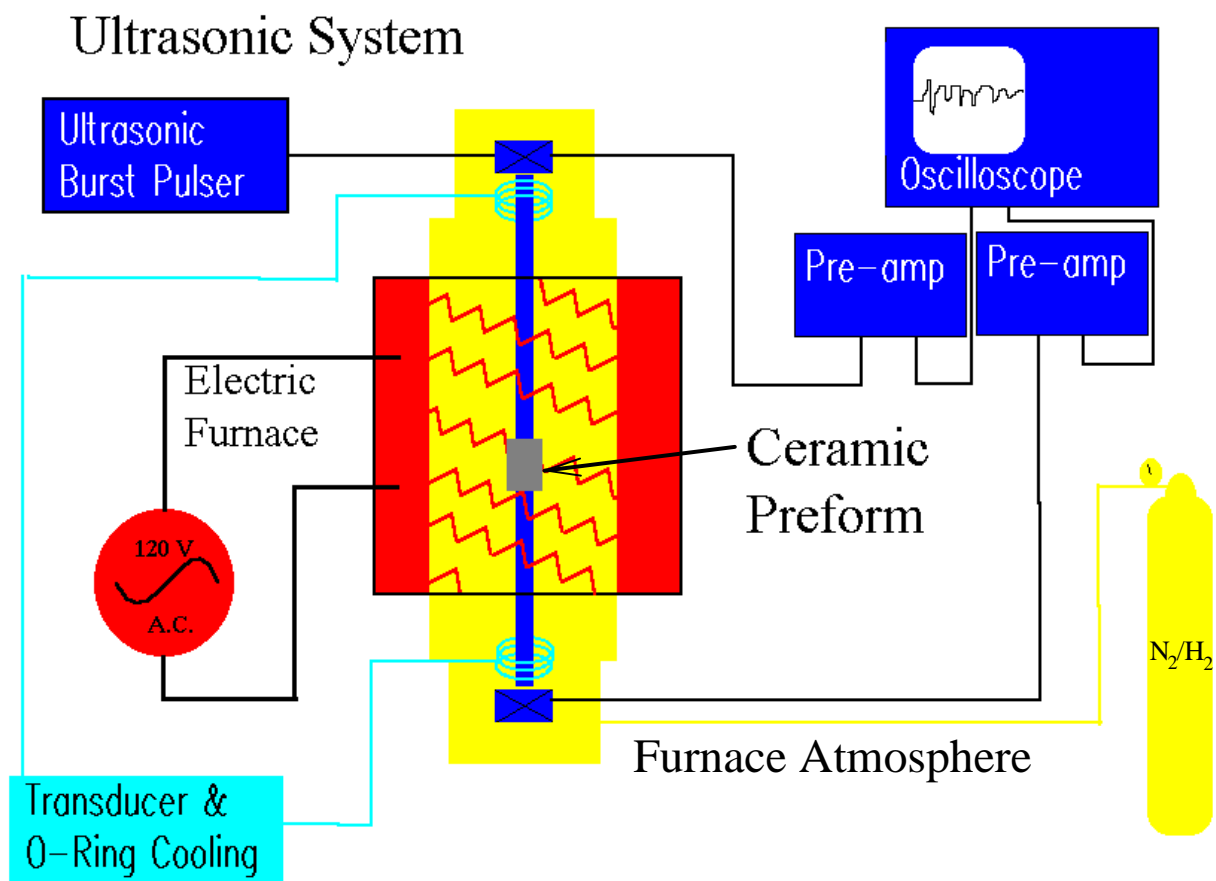


Figure 1: Reaction Bonding System Configuration.

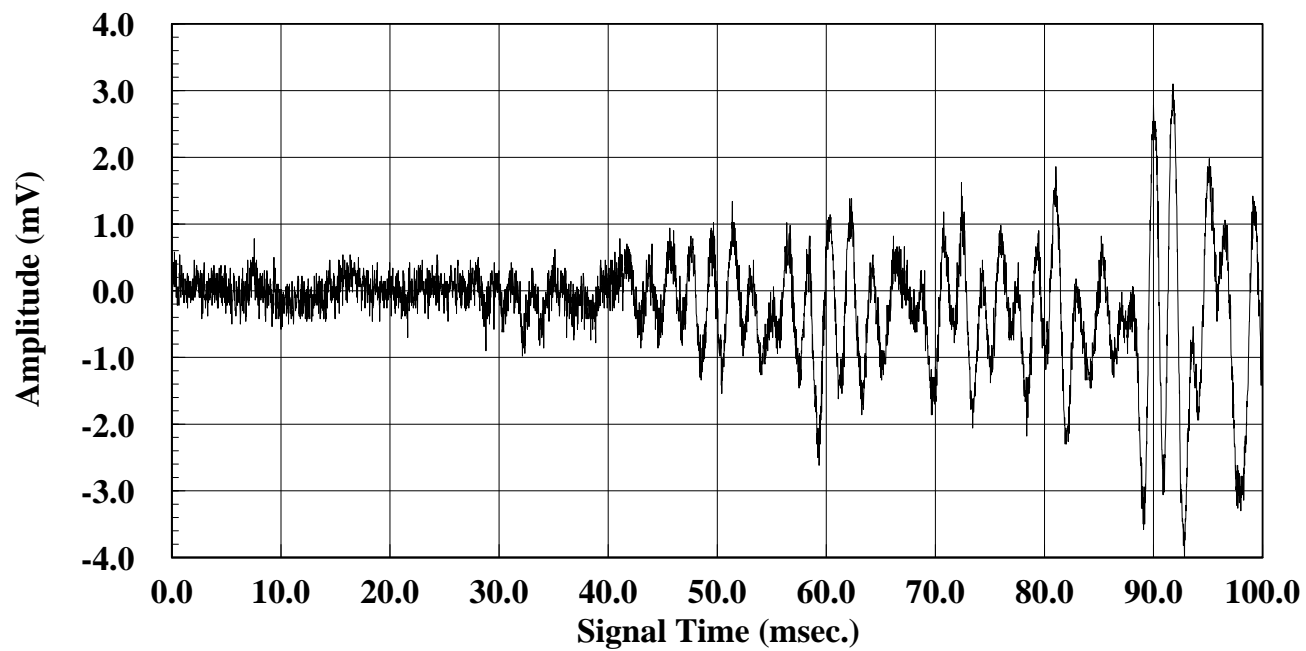


Figure 2: Through transmission ultrasonic signal, unreacted silicon in forming gas, 1250°C.

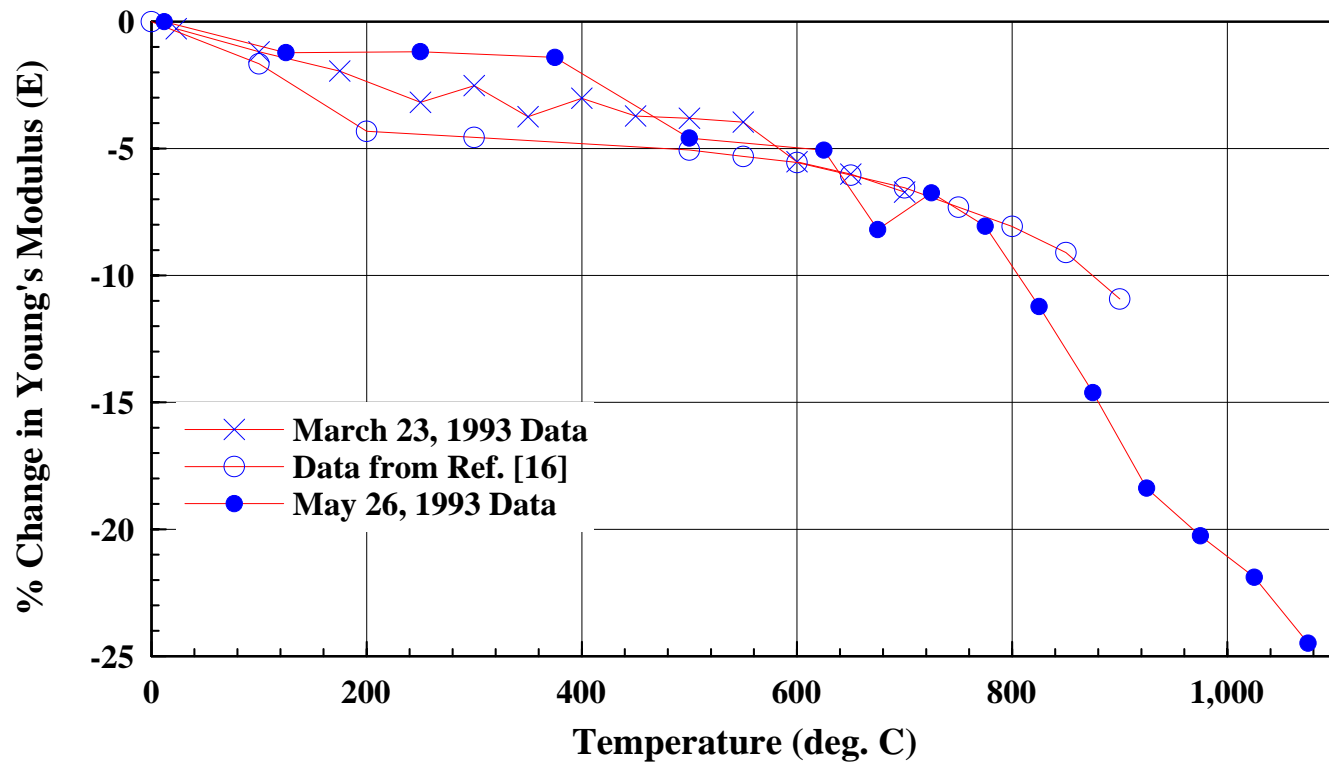


Figure 4: Change in elastic modulus from heating of polycrystalline nickel.

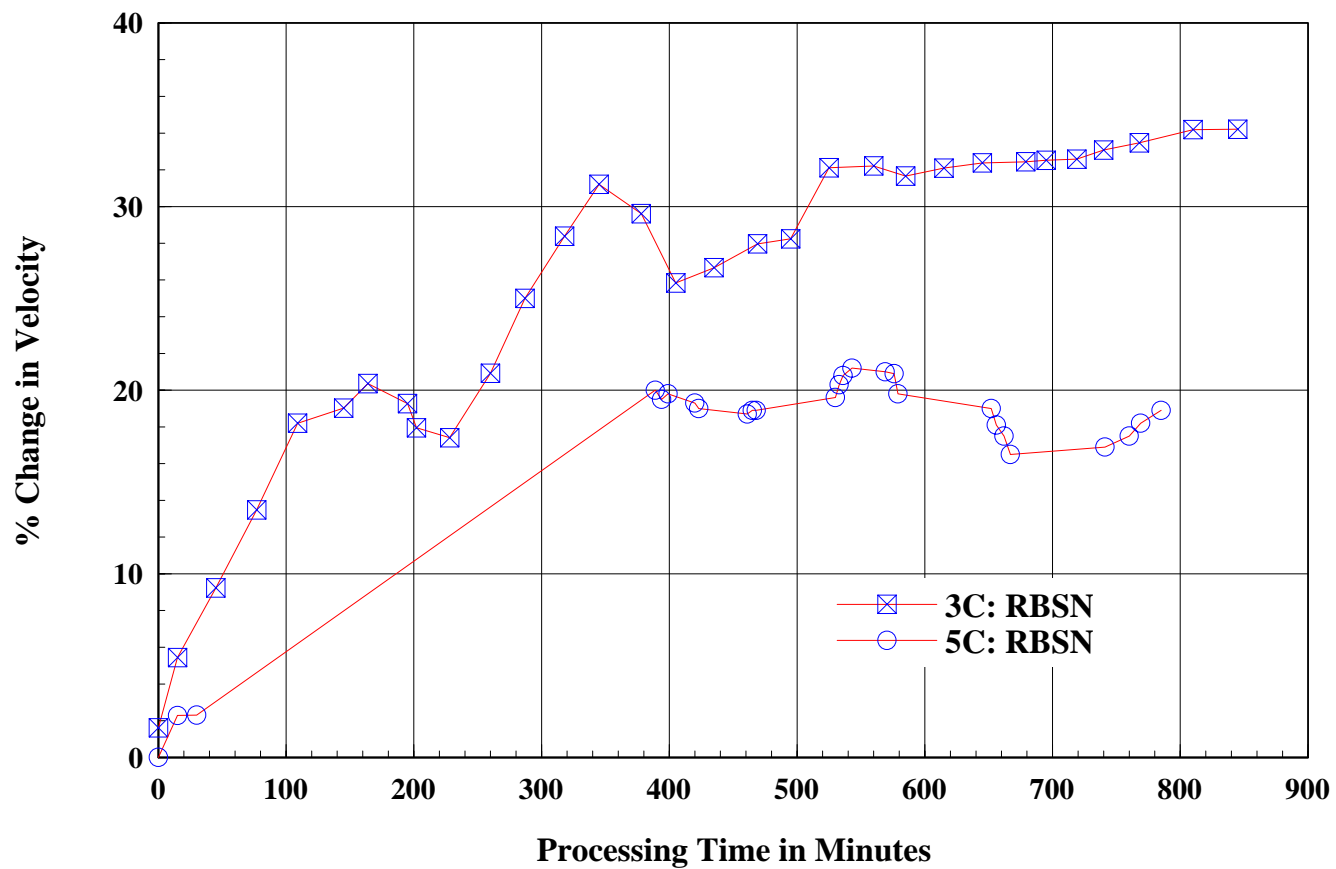


Figure 7: Change in ultrasonic velocity during reaction bonding of silicon nitride.

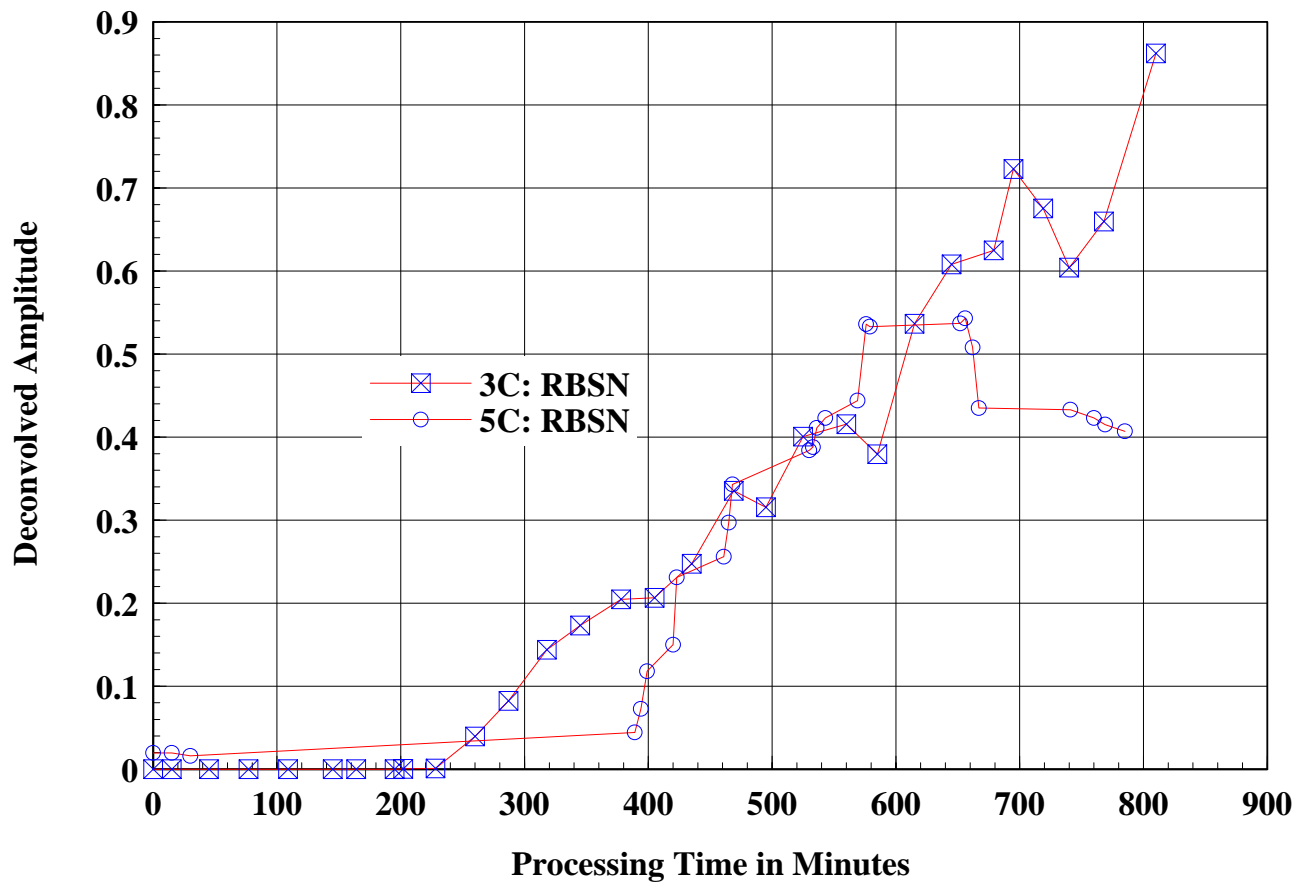


Figure 8: Change in amplitude of ultrasonic signal during reaction bonding of silicon nitride.

Figure 1: Reaction Bonding System Configuration.

Figure 2: Through transmission ultrasonic signal, unreacted silicon in forming gas, 1250°C.

Figure 3. Six signals acquired from the monitoring system.

Figure 4: Change in elastic modulus from heating of polycrystalline nickel.

Figure 5: Magnitude scalograms from through transmission signals from early in the processing (top) and late.

Figure 6: Magnitude and phase scalograms from through transmission signal, magnitude surface and contours, phase contours only.

Figure 7: Change in ultrasonic velocity during reaction bonding of silicon nitride.

Figure 8: Change in amplitude of ultrasonic signal during reaction bonding of silicon nitride.